

Peptide-Based Glioma-Targeted Drug Delivery Vector gHoPe2

Elo Eriste,^{#,†} Kaido Kurrikoff,^{*,#} Julia Suhorutšenko,[†] Nikita Oskolkov,[†] Dana Maria Copolovici,[†] Sarah Jones,[‡] Pirjo Laakkonen,^{§,¶} John Howl,[‡] and Ülo Langel^{†,||}

[†]Institute of Technology, University of Tartu, Estonia

[‡]Research Institute in Healthcare Science, School of Applied Sciences, University of Wolverhampton, United Kingdom

[§]Research Programs Unit, Molecular Cancer Biology, and Institute of Biomedicine, University of Helsinki, Finland

[¶]Foundation for the Finnish Cancer Institute, Finland

^{||}Department of Neurochemistry, Stockholm University, Sweden

S Supporting Information

ABSTRACT: Gliomas are therapeutically challenging cancers with poor patient prognosis. New drug delivery strategies are needed to achieve a more efficient chemotherapy-based approach against brain tumors. The current paper demonstrates development of a tumor-targeted delivery vector that is based on a cell-penetrating peptide pVEC and a novel glioma-targeting peptide sequence gHo. The unique tumor-homing peptide gHo was identified using *in vitro* phage display technology. The novel delivery vector, which we designated as gHoPe2, was constructed by a covalent conjugation of pVEC, gHo, and a cargo; the latter could be either a labeling moiety (such as a fluorescent marker) or a cytostatic entity. Using a fluorescent marker, we demonstrate efficient uptake of the vector in glioma cells and selective labeling of glioma xenograft tumors in a mouse model. This is the first time that we know where *in vitro* phage display has yielded an efficient, *in vivo* working vector. We also demonstrate antitumor efficacy of the delivery vector gHoPe2 using a well-characterized chemotherapeutic drug doxorubicin. Vectorized doxorubicin proved to be more efficient than the free drug in a mouse glioma xenograft model after systemic administration of the drugs. In conclusion, we have characterized a novel glioma-homing peptide gHo, demonstrated development of a new and potential glioma-targeted drug delivery vector gHoPe2, and demonstrated the general feasibility of the current approach for constructing cell-penetrating peptide-based targeted delivery systems.



■ INTRODUCTION

Tumors represent the most common cause of death in humans. Of the three main anticancer interventions—irradiation, surgery, and systemic treatment—chemotherapy is currently the principal antineoplastic treatment in the clinic. However, chemotherapy lacks specificity toward tumor cells and is thus highly toxic to normal tissues. Accordingly, current endeavors are focused on enhancing the specificity of chemotherapy.¹

Some cancer types are more effectively treated by chemotherapy, while others are not. For example, treatment of brain tumors is especially difficult because surgery is not feasible and chemotherapy is ineffective. Gliomas are aggressive brain tumors and therapeutically very challenging cancers. Prognosis of glioblastoma patients is poor with a median survival of less than 1 year and only a 3% chance of survival beyond two years.² Gliomas are primarily challenging to treat owing to the pharmacokinetic limitations of commonly used low-molecular-weight chemotherapeutics (the drug is cleared before it reaches brain parenchyma).³ Drug delivery to the most distant glioma cells, which are behind the blood-brain barrier, is limited by insufficient penetration of systemically administered drugs.

Therefore, novel approaches to increase the specificity of chemotherapy and increase the treatment efficacy for brain tumors are needed. During recent years, a widely studied strategy is to alter the pharmacokinetics of chemotherapeutics by incorporating the drug molecule into a delivery vehicle and/or shift the pharmacodynamics by adding targeting properties.⁴

One way of adding targeting properties to the drug molecule is derivatizing it with a selective tumor-binding moiety, such as an antibody, receptor ligand, or homing peptide. Tumor homing peptides⁵ arise from large-scale screening of peptide libraries and subsequent selection of individual peptides that selectively bind to tumor cells and not to normal tissues. The main drawback with most homing peptides, however, is their inability to penetrate the interior of tumors (for example, see ref 6). In order to confer cellular uptake of homing peptides, further derivatization is warranted by the incorporation of a cell-penetrating peptide (CPP).⁷

Received: July 6, 2012

Revised: January 24, 2013

Published: January 28, 2013

CPPs⁸ are promising delivery vehicles, with the distinctive advantages of high cellular uptake and low intrinsic toxicity.⁹ CPPs constitute a relatively new class of transport vector that has received increasing attention during recent years. These cationic and/or amphipathic peptides are usually less than 30 amino acids in length and have the ability to rapidly translocate into most mammalian cells. The utility of these peptides arises from their ability to internalize various cargo molecules such as drug molecules, oligonucleotides, peptides, proteins, plasmids, liposomes, and nanoparticles, both *in vitro* and *in vivo*.¹⁰

We are currently presenting a potential application for CPPs, namely, the development of a glioma-selective drug delivery vehicle based on a new glioma-specific homing peptide conjugated to a CPP pVEC. We have used an 18-amino-acid-long peptide pVEC, which is one of the well-characterized CPPs,¹¹ suitable for drug delivery research because of its high cell penetrating efficacy and low toxicity.^{12,13} This is the first time that we know of where *in vitro* phage display technique has been successfully used for *in vivo* cancer targeting.

■ EXPERIMENTAL PROCEDURES

Phage Display. U251 glioma cells of human origin were cultured in Dulbecco's Modified Eagle Medium (DMEM) with L-glutamine. Medium was supplemented with 10% (v/v) fetal bovine serum (FBS), penicillin (100 U/mL), and streptomycin (100 µg/mL). U251 cells were incubated with the M13 phage display library (Ph.D.-12 New England Biolabs) at 3.75×10^{10} plaque forming units overnight at 4 °C. Unbound phage were washed away by serial washing in culture medium containing 1% (w/v) bovine serum albumin (BSA). Bound phage were eluted by gentle agitation in 0.2 M glycine-HCl (pH 2.2) containing 1 mg/mL BSA for 10 min and subsequently neutralized with 1 M Tris-HCl (pH 9.1). Cell-specific phage were amplified in *E. coli* and subjected to four rounds of panning according to the manufacturer's instructions (New England Biolabs, UK). High-affinity individual clones were identified by DNA sequencing (AltaBioscience, Birmingham, UK).

Peptide Synthesis. Peptides (Table 1) were synthesized in a stepwise manner at a 0.1 mmol scale on an automated peptide

For the *in vitro* and *in vivo* cellular uptake studies, the peptides were N-terminally labeled with 5(6)-carboxyfluorescein (FAM) (Novabiochem) by treatment of peptidyl-resin with 5(6)-carboxyfluorescein (3 equiv), *N,N'*-diisopropylcarbodiimide (3 equiv), hydroxybenzotriazole (3 equiv), and *N,N*-diisopropylethylamine (6 equiv) in dimethyl sulfoxide (DMSO)/dimethylformamide (1:1) overnight. The final cleavage was performed using a standard protocol (95% trifluoroacetic acid (TFA)/2.5% triisopropylsilane/2.5% water) for 3 h at room temperature.

Peptides were purified by using reversed-phase HPLC fitted with a C18 column (Zorbax 300SB-C18, Agilent) and a gradient of 5–100% acetonitrile/water containing 0.1% TFA for 45 min. The molecular weight of peptides was analyzed by MALDI-TOF mass spectrometry (The Voyager-DE PRO Biospectrometry System) in positive linear mode using α -cyano-4-hydroxycinnamic acid as matrix (Sigma-Aldrich) and purity was more than 95% as determined by analytical HPLC.

For the preparation of doxorubicin conjugates, additional cysteine was added to the N-terminus, followed by the cleavage and purification of the peptides as described above. Doxorubicin was conjugated to peptides as described previously¹⁵ with small alterations. Briefly, doxorubicin (2 mg) was dissolved in 500 µL of DMSO and then dispersed in a phosphate buffer solution (500 µL, pH 8.0) at a concentration of 2 mg/mL. After addition of 20 µL of triethylamine (TEA), 200 µL of succinimidyl-4-(*N*-maleimidomethyl)cyclohexane-1-carboxylate (SMCC, 10 mg/mL) was added. The mixture was incubated at a room temperature for 2 h. After adjusting the pH of the mixture to 5.5 with 2 M HCl, 300 µL of peptide solution (15 mg/mL) was added. The mixture was kept at a room temperature for an additional 2 h. In order to remove free doxorubicin, SMCC, and TEA, the reaction mixture was subjected to reversed-phase purification using a gradient of acetonitrile/water containing 0.1% TFA (5–100% for 45 min). The identity and purity of the obtained conjugates were confirmed by using MALDI-TOF mass spectrometry and analytical HPLC, respectively.

Cell Culture. The human embryonic kidney 293 cell line (HEK 293) and human glioma, epithelial-like cell line U87 MG (American Type Culture Collection via LGC, Sweden) and cervical cancer HeLa cells were cultured in Dulbecco's Modified Eagle Medium (DMEM) with L-glutamine. Medium was supplemented with 10% FBS, sodium pyruvate (1 mM), penicillin (100 U/mL), streptomycin (100 µg/mL), and 1% nonessential amino acids (further denoted as complete medium) (PAA Laboratories GmbH, Austria). Cell cultures were cultivated at 37 °C in a humidified 5% CO₂ incubator.

Flow Cytometry. U87, HEK, and HeLa cells (5×10^4) were seeded 24 h prior to experiments into 24-well plates. Cells were incubated for 30 min in complete media after treatment with the peptide constructs. Thereafter, cells were washed four times with PBS and once with trypsin, suspended in ice-cold PBS, and flow cytometry analysis was carried out with a BD LSR II flow cytometer (BD Biosciences, San Jose, CA, USA) equipped with a 488 nm argon laser and analyzed with FACSDiva software. The filter settings for excitation and emission were 480/530 nm bandpass (FL1) for FITC. Live cells were gated by forward/side scattering from a total of 10 000 events.

Confocal Microscopy. U87 cells (1×10^4) were seeded in Lab-Tek 8-well chamber slides to reach 50% confluence one day prior to experimentation. After 30 min of incubation with

Table 1. Sequences of Peptides

name	sequence
pVEC	LLILRRIRKQAHASK-NH ₂
gHo	NHQQQNPHQPPM-NH ₂
FAM-pVEC	^a LLILRRIRKQAHASK-NH ₂
FAM-gHo	^a NHQQQNPHQPPM-NH ₂
FAM-pVEC-gHo (FAM-gHoPe2)	^a LLILRRIRKQAHASK-NHQQQNPHQPPM-NH ₂
FAM-gHo-pVEC (FAM-gHoPe3)	^a NHQQQNPHQPPM-LLILRRIRKQAHASK-NH ₂
Dox-pVEC-gHo (Dox-gHoPe2)	^b XCLLILRRIRKQAHASK-NHQQQNPHQPPM-NH ₂

^a5(6)-Carboxyfluorescein. ^bDoxorubicin. X: succinimidyl-4-(*N*-maleimidomethyl) cyclohexane-1-carboxylate (SMCC).

synthesizer (Applied Biosystems model 433A) using Fmoc solid-phase peptide synthesis strategy.¹⁴ Rink-amide MBHA (methylbenzylhydramine) resin (MultiSyntech GmbH, Germany) was used as a solid support to obtain C-terminally amidated peptides. All chemicals used in peptide synthesis were purchased from Sigma-Aldrich (Germany), MultiSyntech GmbH (Germany), and Scharlau (Spain).

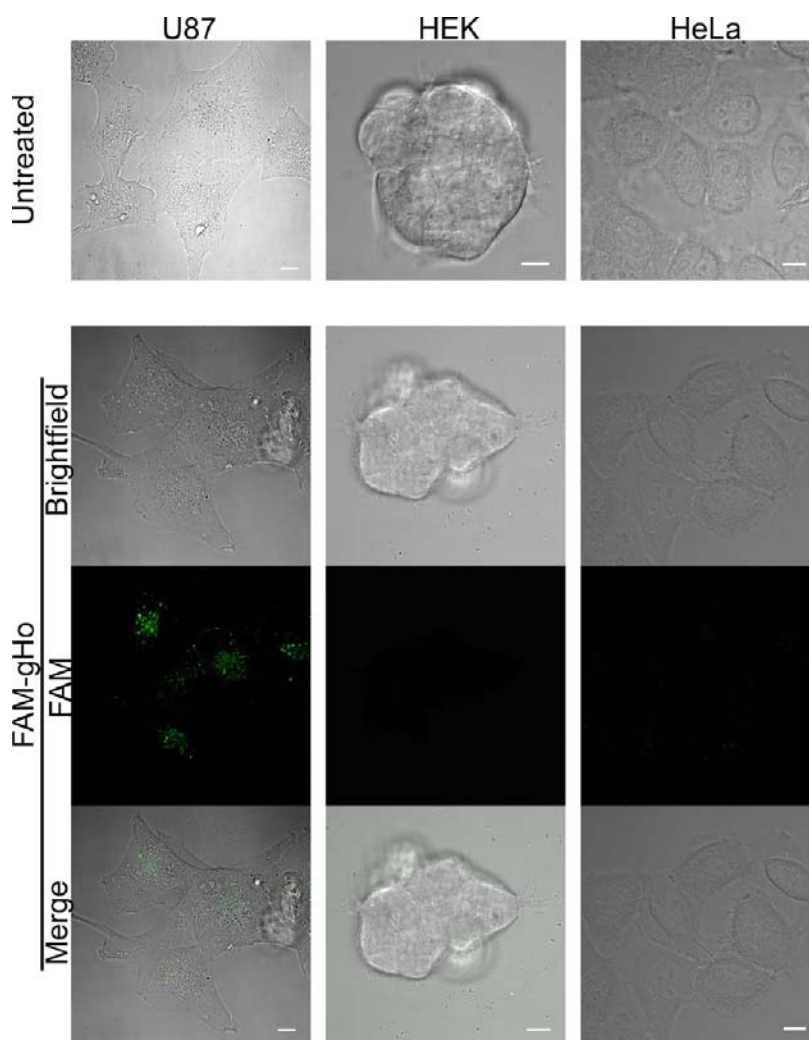


Figure 1. Association of the homing peptide gHo (green) with glioma cells (U87) and with HeLa and HEK cells. The upper row shows untreated cells; peptide treatment is presented in the lower panel. The peptide was applied at a concentration of 20 μ M. gHo associated with U87 cells, but not with HEK and HeLa cells. Scale bar 10 μ m.

the peptide constructs in complete medium at 37 $^{\circ}$ C, cells were washed four times with PBS, followed by the addition of trypan blue (0.1%) in OptiMEM and examined using Zeiss LSM710 (Carl Zeiss GmbH, Germany) inverted microscope equipped with FluoView 1000 confocal system using a 60 \times water-immersion and 100 \times oil-immersion objectives and excitation at 488 nm (fluorescein). For the membrane association experiments, the cells were incubated with FAM-labeled peptide for 30 min at 37 $^{\circ}$ C in complete medium. After the incubation period, cells were washed once with PBS and resuspended in fresh OptiMEM medium.

In Vitro Toxicity. Membrane integrity was evaluated using LDH leakage assay (Sigma-Aldrich, St. Louis, MO, USA), which measures lactate dehydrogenase release. Briefly, 1×10^4 cells were seeded 24 h in 96-well plates before treatment with the peptides or peptide–drug conjugates, which was conducted in complete medium for 48 h. Thereafter, LDH leakage was assessed according to the manufacturer’s protocol. Untreated cells were defined as no leakage, and 100% leakage was defined as total LDH release by lysing cells in 0.2% Triton X-100 in HKR buffer.

Long-term toxicity was evaluated using an MTS proliferation assay (Promega, Madison, WI, USA). The MTS assay measures

the activity of mitochondrial dehydrogenases to convert tetrazolium salts into formazan. Briefly, 1×10^4 cells were seeded in 96-well plates 24 h before treatment with the peptides or peptide–drug conjugates, which was conducted in complete medium for 24 h. Thereafter, MTS proliferation assay was used according to the manufacturer’s protocol. Untreated cells were defined as 100% viable.

Animal Experiments and Post-Mortem Tissue Analysis. Localization of the peptide vectors was assessed post mortem after injecting FAM-labeled peptides in homozygous female nude mice (C.Cg/AnNTac-Foxn1nu, Taconic), bearing tumor xenografts either intracranially or subcutaneously. 8×10^5 U87 cells were resuspended in 100 μ L (s.c. tumor model) or in 5 μ L (intracranial tumor model) of fresh DMEM medium, without serum and antibiotics. The xenografting was performed by implanting the cell suspension subcutaneously or intracranially into one of the striatum (stereotaxic coordinates $A = +1$, $L = +2$, $V = +3.5$). At the appearance of the first signs of tumor growth (for the subcutaneous tumors, tumor size of approx 300 mm³; for the intracranial tumors, the first sign is usually weight loss), mice were injected i.v. (via tail vein) with the peptide constructs. For the biodistribution, 100 μ L of 200 μ M FAM-labeled peptide suspension (in saline) was used. This

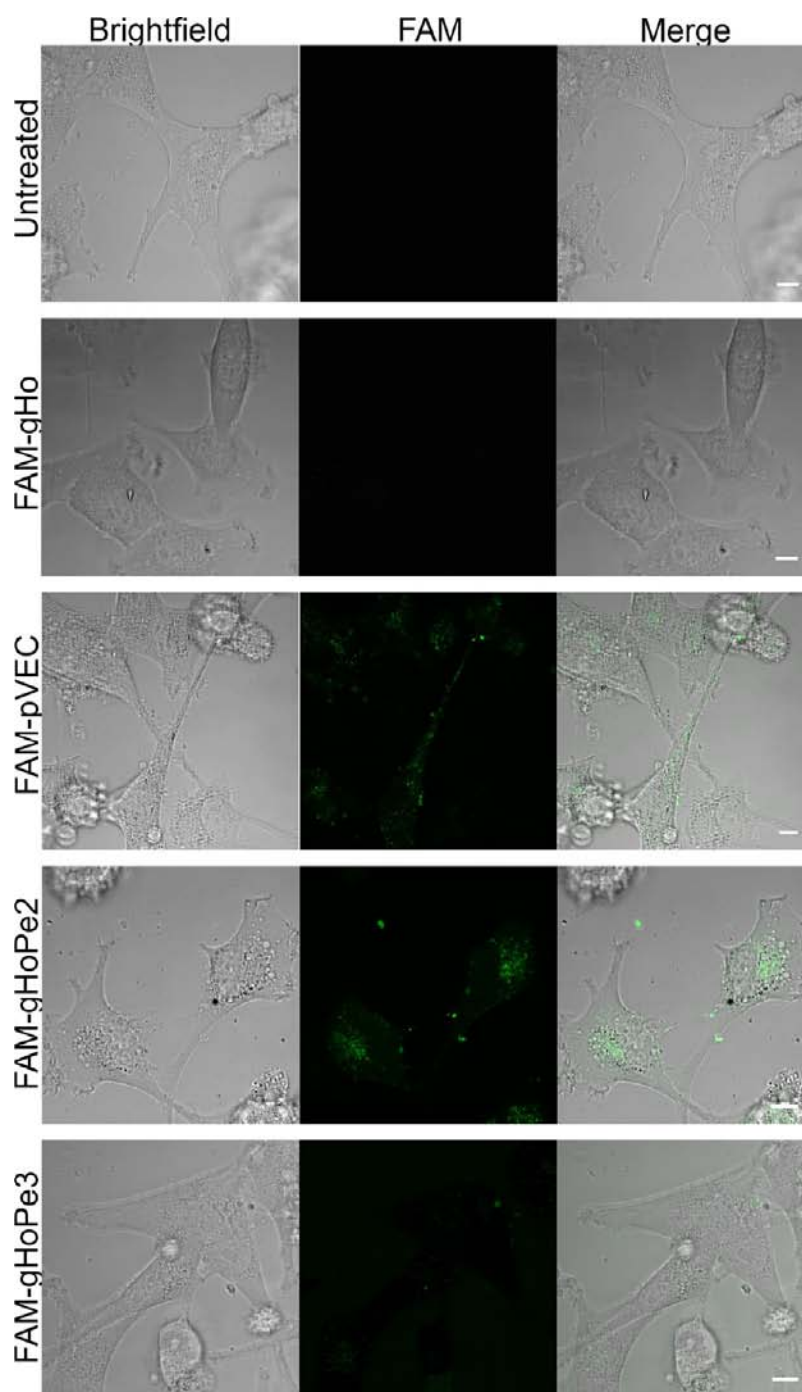


Figure 2. Cellular internalization of pVEC in different C- and N-terminal configurations with the homing sequence gHo, labeled with FAM (green), in U87 glioma cells. All peptides were applied at a concentration of 10 μ M. Free homing peptide gHo showed no uptake, while pVEC, gHoPe2, and gHoPe3 exhibited cellular uptake of varying degrees.

represents a dose of 4 mg/kg for a mouse of 20 g. At 3 h postinjection, the animals were anesthetized and intracardially perfused with 50 mL of PBS, followed by 50 mL of fixation solution (4% w/v paraformaldehyde in PBS, pH 7.4). Tissues were collected, postfixed for 2 h in the same fixation solution, cryoprotected in sucrose (10% for 24 h, followed by 30% for 1 week, at 4 °C), snap-frozen in 2-methylbutane (AppliChem) kept on dry ice. The tissues were cut on a cryostat with a thickness of 10–15 μ m, counterstained with DAPI (AppliChem), and mounted using Vectashield (Vector Laboratories) mounting media.

The tumor treatments were performed using 1 mg/kg doxorubicin (369 μ M, 100 μ L, for an animal of 20 g) and an equivalent dose (8.3 mg/kg) of dox-gHoPe2 (369 μ M, 100 μ L) i.v. twice a week. The subcutaneous tumor dimensions were measured using calipers; tumor volume was calculated as $(\text{length} \times \text{width}^2)/2$. A mixture of ketamine 75 mg/kg (Vetoquinol, Bioketan) and dexmedetomidine (Laboratorios SYVA, Dorbene) 1 mg/kg i.p. in saline was used for the anesthesia. After surgery, the anesthesia was blocked using the α_2 -adrenergic antagonist atipamezole hydrochloride (Antisedan), 1 mg/kg s.c. All the animal procedures and experiments

were approved by the Estonian laboratory animal ethics committee (approvals no. 19, dated Sep 25, 2009, nos. 69 and 70, dated Feb 9, 2011).

Statistics. All figures are presented as mean \pm SEM. The cell uptake data represent three independent experiments performed in duplicate. For toxicity measurements, a decrease in viability was considered significant at $p < 0.001$ using ANOVA Dunnett's multiple comparison test.

RESULTS

Construction of the Delivery Vector. To find new peptide sequences which effectively bind glioma cells, we utilized a phage display technique on U251 glioma cells, a pH12 M13 phage display library and four rounds of panning. From the screen, one clone was sequenced, yielding a 12-amino-acid sequence NHQQQNPHQPPM-NH₂. We subsequently refer to this peptide as "gHo" (an acronym of words representing glioma-homing).

To confirm binding of the homing peptide with glioma cells, gHo peptide was labeled with FAM and incubated with U87 glioma cells as well as with two non-neuronal cell lines, HeLa and HEK, for 30 min at the room temperature, followed by mild washing of the cells, for estimating cell membrane binding and cellular uptake. Confocal microscopy confirmed the fluorescence from FAM-gHo only in U87 cells (Figure 1, small magnification image in Figure S1, Supporting Information) at all the tested concentrations (5–20 μ M of the peptide). gHo did not bind to HeLa and HEK cells even at the very high concentration of 20 μ M. Although the fluorescent signal was not very high, there was a clear distinction between the presence of signal in U87-s and absence in other cell types. It should also be noted that, when thorough washing of the cells was performed (such as for estimation of cellular uptake, Figure 2), all fluorescence was also removed in U87 cells, suggesting that gHo does not internalize the cells, but binds to cell membranes.

Next, we generated a series of putative delivery vectors, consisting of the tumor-homing peptide gHo, CPP, and a cargo (Table 1). For the vectorization of gHo, a CPP pVEC and covalent conjugation was used. Initially, a fluorescent marker was chosen as a test cargo. The chimeric peptide sequences of FAM-pVEC-gHo and FAM-gHo-pVEC, as well as the control peptides are presented in Table 1. For the sake of convenience, the chimeric sequence pVEC-gHo is subsequently designated "gHoPe2" and the sequence gHo-pVEC as "gHoPe3" (acronyms of words representing glioma-homing peptide).

Cellular Uptake. To confirm that the CPP-activity is not hampered by conjugation of gHo and a cargo with pVEC, cellular uptake of the chimeric peptides gHoPe2 and gHoPe3 was assessed qualitatively using confocal microscopy (Figure 2; small magnification image in Figure S2, Supporting Information) and quantitatively using flow cytometry (Figure 3) in U87 cells. The free homing peptide gHo did not internalize in U87. As anticipated, the unmodified pVEC internalized very efficiently in the U87 cells. FAM-gHoPe2 showed similar internalization efficiency as pVEC, while the FAM-gHoPe3 internalized but to a lesser extent (Figure 2).

Quantitative comparison of the uptake efficacies (Figure 3) was in accordance with the microscopic observations. All the pVEC-based constructs showed high cellular uptake, while free gHo did not internalize. Statistical analysis showed ANOVA interaction between concentration and vector ($F_{(15,145)} = 6.0$, $p < 0.001$). The uptake of FAM-gHoPe2 significantly differed

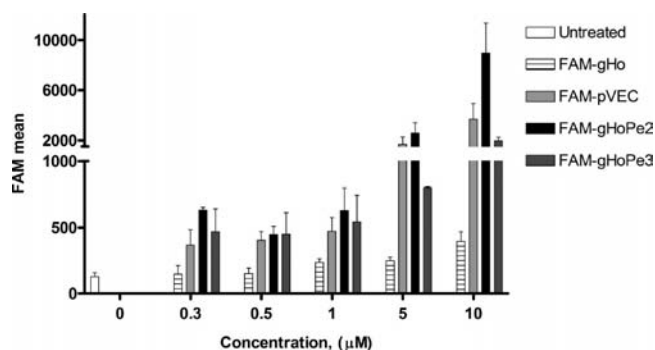


Figure 3. Cellular internalization of pVEC in different C- and N-terminal configurations with the homing sequence gHo, labeled with FAM (green), measured by FACS. Overall, the uptake of pVEC and gHoPe2 was highest in the U87 cells.

from the uptake values of FAM-gHoPe3 (main effect $p < 0.01$, Tukey post hoc) and FAM-gHo ($p < 0.001$).

Biodistribution of gHoPe2 in Vivo. Given that the in vitro quantitative uptake analysis demonstrated enhanced propensity of FAM-gHoPe2 for cellular penetration, this construct was subsequently selected for the in vivo studies. The biodistribution of FAM-labeled gHoPe2 was therefore determined. First, we used a mouse model of subcutaneous U87 tumor. FAM-labeled gHo and gHoPe2 were injected 3 h before tissue collection. The circulation time of 3 h was chosen, since in the initial pilot experiments with 1, 3, 6, and 24 h circulation times, 3 h showed the highest fluorescence in the tumor. Intravenous (i.v.) injection of FAM-labeled constructs in mice bearing subcutaneous tumors and subsequent post-mortem histological analysis showed homing of the FAM-gHoPe2 to the tumor tissue (Figure 4). We detected no FAM-labeled gHo in tumor tissue and none of the peptides in the (intact) brain tissue, kidney, and liver.

Second, biodistribution of FAM-labeled gHo and gHoPe2, as well as FAM-labeled pVEC and gHoPe3, was assessed in a mouse model of intracranial glioblastoma. To estimate the general distribution of gHoPe2 within the glioma-containing brain, the whole coronal section was reconstructed from single microscopic images. Cranial localization of gHoPe2 was seen in the tumor areas but not in the adjacent intact brain (Figure 5).

Closer examination of different tissues confirmed specific localization of gHoPe2 (Figure 6), but not gHoPe3, pVEC, and gHo in tumor tissue (Figure S3 in Supporting Information). gHoPe2 was the only peptide present in the intracranial tumors, but not in adjacent intact brain, kidney, and liver. The other peptides could not be detected in any of the organs.

We also assessed the uptake of the constructs in other tissues. No uptake of gHoPe2, gHoPe3, gHo, or pVEC was seen in lungs, heart, spleen, muscle, and skin (Figure S4 in Supporting Information).

Cytostatic Effect in Vitro. Before conjugation of the vector with the chemotherapeutic molecules, we tested the effect of the gHoPe2 on cell viability. pVEC, gHoPe2, and gHoPe3 did not affect cell viability even at very high concentrations of 20 μ M (Figure S5 in Supporting Information).

gHoPe2 was chosen for subsequent assessment of potential use as a vector for systemic delivery of an anticancer drug. For this, doxorubicin was covalently conjugated with gHoPe2 (Table 1, Figure S6 in Supporting Information) and its cytotoxic efficacy was analyzed. Free doxorubicin had a clear effect on cell viability, with even low doses exerting quite large

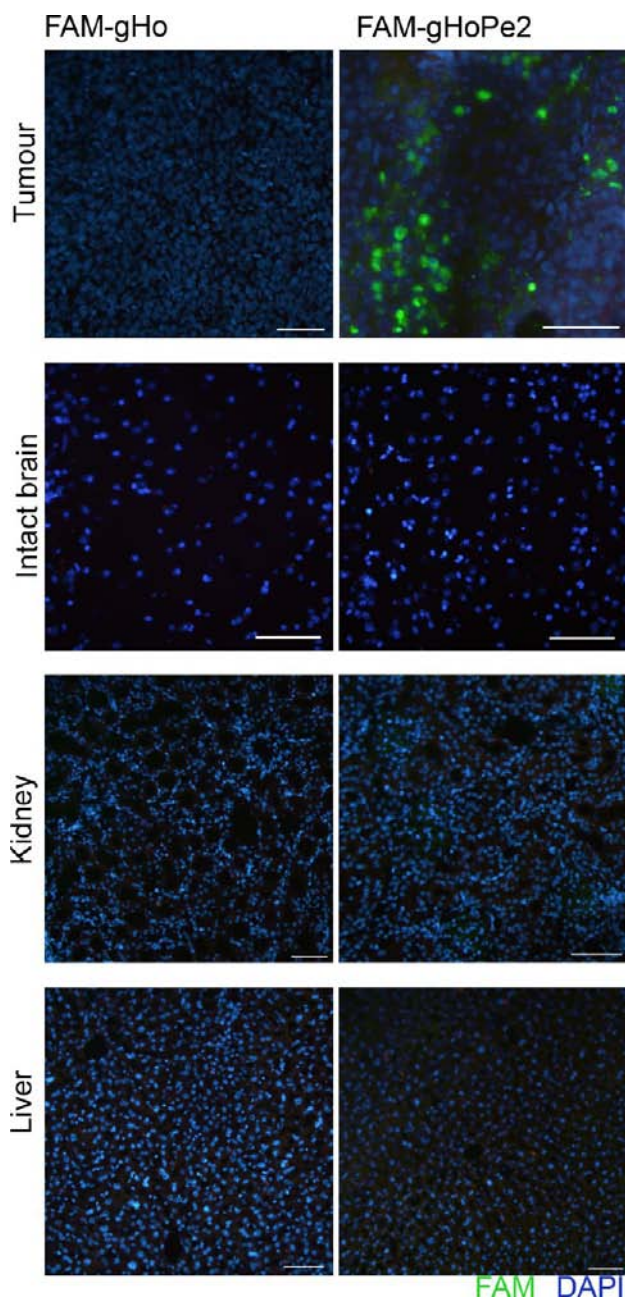


Figure 4. Localization of FAM-labeled gHo and gHoPe2 in subcutaneous U87 tumors. Labeled peptides were administered i.v. 3 h before tissue collection. Cryosections from the subcutaneous tumors, as well as from brain, kidney, and liver were counterstained with DAPI and visualized by fluorescent microscopy. gHoPe2 (green) localized in tumors. FAM and DAPI are merged in the images. Scalebar 100 μ m.

toxic effect (Figure 7). Dox-gHoPe2 exerted similar cytotoxic effects as the free drug.

Antitumor Effect in Vivo. The efficacy of dox-gHoPe2 was assessed in the model of subcutaneous U87 tumors, as the tumor growth can be easily monitored. The treatment was commenced when visible tumors (approx. 300 mm³) had developed. The animals were randomized into three treatment groups; animals receiving either free doxorubicin (1 mg/kg (369 μ M, 100 μ L, for an animal of 20 g), dox-gHoPe2 (8.3 mg/kg (369 μ M, 100 μ L) i.v. twice a week, or no treatment (i.v. injection of saline). Tumor sizes were recorded twice a week. Repeated-measures ANOVA of the tumor growth dynamics

(Figure 8) showed significant treatment main effect ($F_{10,65} = 2.1$, $p < 0.05$), the tumors in dox-gHoPe2 group being significantly smaller from the tumors in the untreated group (Tukey posthoc $p < 0.05$).

Finally, dox-gHoPe2 was also administered to animals with intracranial gliomas, using similar experimental setup as in the subcutaneous tumor model. The animals received two 1 mg/kg injections of doxorubicin per week, or an equivalent molar amount of dox-gHoPe2. We monitored both body weight loss and survival of the animals. Although the loss of body weight was somewhat smaller in the group receiving dox-gHoPe2 (Figure S7 in Supporting Information), it was not large enough to reach statistical significance. The treatment with either free dox or dox-gHoPe2 did not prolong the survival of the animals.

DISCUSSION

We have developed a tumor-specific carrier peptide that may have utility in several applications, such as for selective labeling of tumors or, in conjunction with an anticancer moiety, as a cytostatic drug. The vector is based on a combination of a tumor-homing peptide and a CPP. The underlying rationale and potential behind this approach is to enhance delivery of chemotherapeutic molecules by conjugating them to CPPs. Since CPPs in general do not prefer specific cell types, the homing sequence provides a means of targeting the CPP toward desired cells or tissues.

The onset of this study entailed phage selection and characterization of a new glioma-specific peptide sequence (homing peptide), which we have designated as “gHo”. Phage display is a useful method for finding new sequences with high affinity toward target cells. Several different tumor homing peptides have been characterized using this method, such as human breast cancer selective peptides PEGA,^{6,7} CREKA,¹⁶ and tumor lymphatics-binding peptide LyP-1,¹⁷ as well as a recent report of glioma-binding peptide CGKRR.¹⁸ These peptides serve as valuable tools that can be used in different applications. Similarly, the new sequence gHo is a useful tool for specifically targeting human gliomas. The glioma-specific targeting of gHo is supported by current in vitro data about association of the peptide with U87 cells, but not with two non-neuronal cell lines HeLa or HEK. In addition, different glioma cell lines were utilized in phage display and subsequent in vitro characterization steps, with the aim of characterizing a general glioma homing sequence, rather than a sequence specific for one particular glioma cell line. Thus, both in vitro and in vivo data demonstrate specific homing of gHo-containing peptide vector intracranial and subcutaneous glioma.

The choice of the CPP is based on previous positive results, where pVEC was shown to be an efficient CPP in vitro^{12,13} and in vivo.⁷ Previously, a similar strategy of combining pVEC with a tumor-homing peptide has been characterized⁷ and used the breast tumor binding peptide sequence PEGA. The conjugate PEGA-pVEC showed accumulation in tumor tissue. Vectorizing a chemotherapeutic drug with this construct increased the potency of the drug in vitro.⁷ Data presented herein employ a similar pVEC-based vector, with a different targeting moiety, and thus demonstrate the utility of the homing peptide–CPP conjugation strategy as a universal vector platform.

The homing sequence gHo and the CPP pVEC were conjugated in two possible ways, the CPP being conjugated to gHo either C- or N-terminally (resulting in a construct where the CPP is situated either between the cargo and gHo (gHoPe2), or at the terminal position (gHoPe3), respectively).

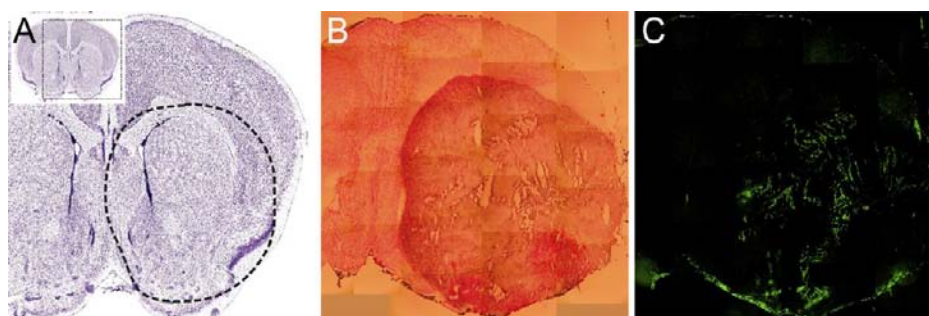


Figure 5. Coronal section of a mouse brain with U87 tumor in the right striatum, Bregma +1 mm. (A) A Nissl-stained reference section (Allen Institute, <http://mouse.brain-map.org>) of a normal mouse brain at the same level and size where tumor sections B and C are viewed. The respective tumor area is circled with a dotted line. The inset shows the whole coronal section. (B) H&E stained hemisphere of brain and glioma, reconstructed from single microscopic images. The animals received an i.v. injection of FAM-labeled gHoPe2 3 h before tissue collection. (C) Fluorescence image from the same location (reconstructed from single fluorescence microscopic images), indicating global FAM localization in the tumor area.

The main aim of the cellular uptake studies was to confirm that the cell penetrant properties of the conjugates were retained after addition of gHo and the cargo. Intriguingly, the gHoPe2 construct showed higher cellular uptake, compared to gHoPe3, where the CPP is terminally exposed. Moreover, *in vivo* data also confirmed higher tissue uptake of gHoPe2. One would assume that, if there were differences in uptake efficacies, gHoPe3 would be more efficient, because of the exposure of the CPP moiety, allowing better contact with the cell membrane. On the other hand, we have not studied the physicochemical parameters of the chimeric conjugates in aqueous solution, as well as the effect of adding salts (as in case of using saline). It is possible that the conjugates interact with each other and/or with the components of the solution and the solution may not be composed of monomer conjugate elements, which in turn means that the effect of the CPP position in the chimeric molecule may not be entirely intuitive. This aspect is rarely studied in similar studies. Nevertheless, both gHoPe2 and gHoPe3 constructs were able to internalize in U87 cells and, especially in case of the gHoPe2, we had the basis to proceed with *in vivo* experiments and test its potential use as a targeted drug delivery agent.

The first *in vivo* biodistribution studies were performed using a simplified U87 tumor model, where the tumor cells are implanted subcutaneously. The unvectorized gHo sequence did not localize in tumor, nor did we see any localization in brain, liver, and kidney. This shows that targeting properties without cell penetration (such as with the gHo peptide) is probably not sufficient for effective tissue labeling, which is dependent on several factors like penetration through blood-brain barrier, tissue, and cell penetration. In contrast, gHoPe2 showed considerable localization in tumors, but no localization in brain, liver, and kidney. This prompted us to move further and use a more relevant intracranial tumor model.

The main aim of the study was to target brain tumors. The rationale for this arises from the inefficacy of traditional chemotherapeutics against these types of malignancies. Doxorubicin, although one of the most efficient chemotherapeutics available, is not efficient against brain tumors, mostly because of low penetration through the blood-brain barrier.³ Therefore, the treatment of brain tumors is especially difficult, because surgery is not feasible and chemotherapy is ineffective. Novel strategies for the treatment of brain tumors are therefore imperative. The greatest challenge which now lies ahead is achieving penetration of the blood-brain barrier and selective targeting of the tumor tissue/cells. We therefore also

assessed localization of gHoPe2 in a model of intracranial glioma. The localization of gHoPe2 was in accordance with the subcutaneous tumor model, showing tumor uptake, but no localization in intact brain, liver, and kidney. We also assessed localization of FAM-pVEC, FAM-gHo, and FAM-gHoPe3. All of these failed to label the tumor. In addition, we analyzed the localization of all the constructs in other major tissues: lungs, heart, liver, kidney, spleen, muscle, and skin, but found no evidence of the peptides accumulating in any of the tissues, thus supporting the targeted delivery of gHoPe2.

Finally, we performed a pilot study for assessing the treatment efficacy of gHoPe2 by conjugating the vector to a known and efficient chemotherapeutic drug doxorubicin. We validated the cytotoxic effect of the vectorized doxorubicin, which was identical to the free drug. This is not surprising, because, unless we consider drug resistance mechanisms, both free and vectorized doxorubicin should readily reach the cell interior *in vitro*. However, our hypothesis was that dox-gHoPe2 would have an advantage *in vivo*. Similarly, we used a subcutaneous tumor model, because it allows easy physical monitoring of tumor growth and antitumor effects of the drug. We chose a low dose of doxorubicin, 1 mg/kg twice a week, and compared the effect with an equivalent dose of dox-gHoPe2. While free doxorubicin had a moderate effect on the tumor growth, the effect was greater in the group of animals who received the vectorized drug, dox-gHoPe2, again confirming the efficacy of the delivery vector.

Unfortunately, the results were not as promising for the intracranial tumor model, where administration of dox-gHoPe2 did not prolong the survival of the animals. However, the free doxorubicin did not improve the survival, either. We hypothesize that the used dose—1 mg/kg of doxorubicin equivalent—was too low for having any effect on tumor growth. It is noteworthy that both free and vectorized doxorubicin did not induce regression of tumor in the other tumor model—subcutaneous tumor—either, and did not reduce the tumor volume, but only inhibited the growth. Therefore, we have to consider that higher amounts are required to achieve tumor regression and an effect on survival in intracranial tumor model, because it is known that the brain levels of free doxorubicin are low after *i.v.* injection.^{3,19} Hence, more optimization should be carried out to verify the usefulness of the peptide vector for the treatment of intracranial tumors.

An aspect that has not been currently assessed, but should also be addressed in further studies, is the delivery efficacy of gHoPe2 in glioma cells with different sensitivity/resistance

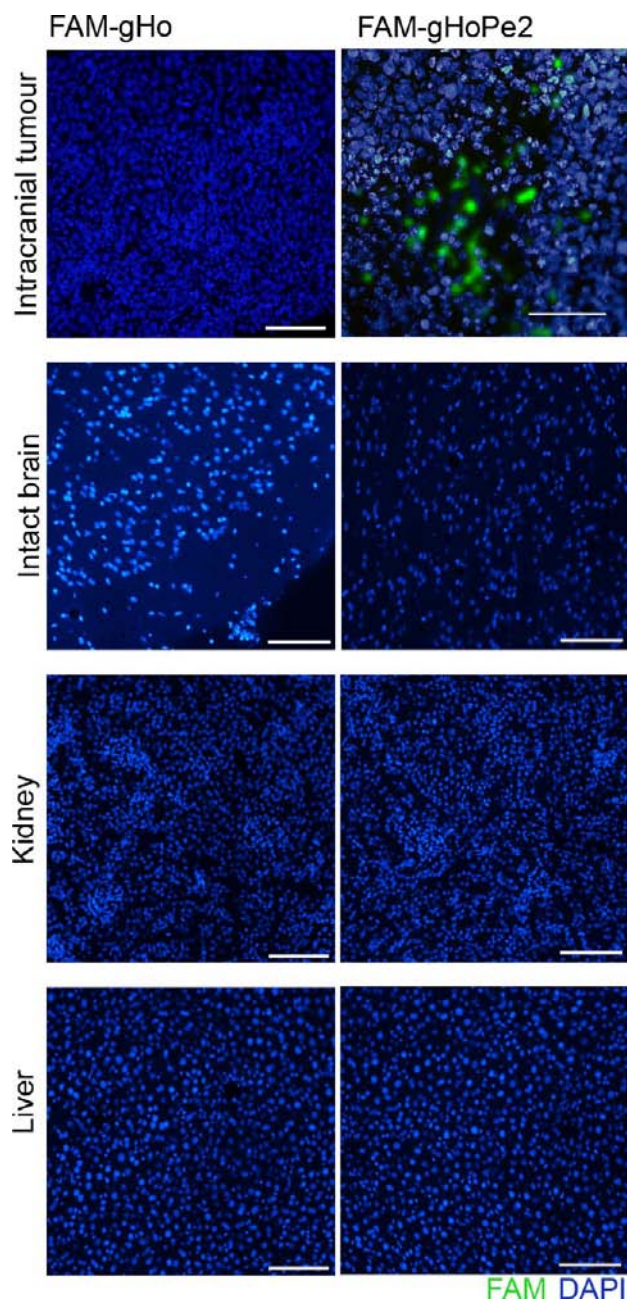


Figure 6. Localization of FAM-labeled gHo and gHoPe2 in intracranial gliomas and intact brain, as well as in liver and kidney. gHoPe2 (green) localizes in tumors. Scale 100 μm .

toward chemotherapy. Overcoming drug resistance, using a CPP vectorization strategy, has previously been demonstrated,^{7,20} and it could be hypothesized that the current vector proves to be effective in this aspect.

There are minimal publications that demonstrate the development of a vector system for the effective systemic treatment of gliomas. Very recently, Erkki Ruoslahti's group has achieved just this,¹⁸ using a new tumor-homing/tumor-penetrating peptide. However, a rarity of studies that have vectorized chemotherapeutics and successfully treated brain tumors indicate that the solutions to the task may not be easy.

The current paper demonstrates a potential application of CPPs for the treatment of tumors. The study combines the approaches of phage display for finding novel peptide

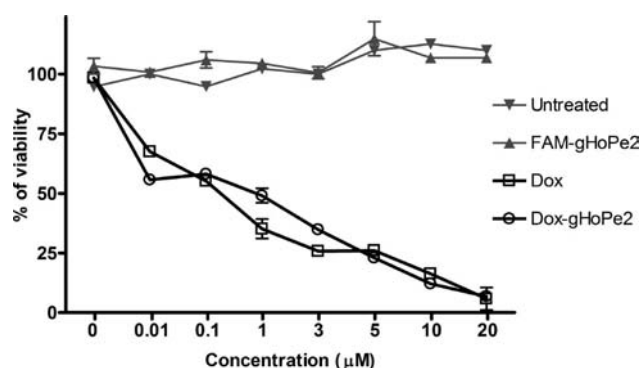


Figure 7. Effect of doxorubicin, dox-gHoPe2, and FAM-gHoPe2 in the viability of U87 cells according to the MTS assay. The constructs were incubated at different concentrations for 24 h. Cells in untreated cultures were defined as having 100% viability.

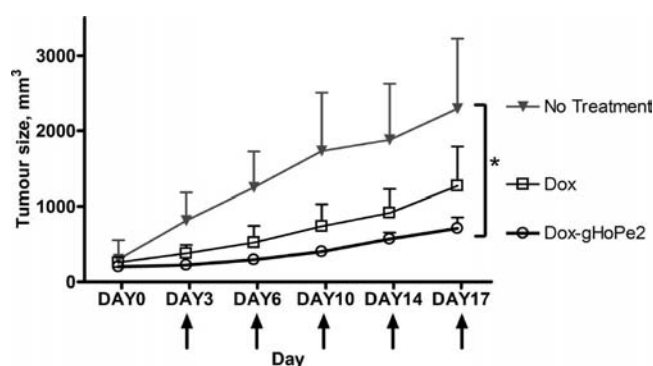


Figure 8. U87 subcutaneous tumor growth dynamics after treatment with either free doxorubicin (i.v. 1 mg/kg twice a week) or with an equivalent molar dose of dox-gHoPe2 (treatment days indicated with arrows). Star represents Tukey posthoc comparison of treatment groups after significant repeated-measures ANOVA. * $p < 0.05$.

sequences that selectively bind to specific tissues or cells and CPPs for ensuring cellular uptake of the cargo. Effective and specific localization of the vector to the glioma was demonstrated *in vivo*, proving, for the first time that we know, successful *in vivo* utilization of *in vitro* phage display for cancer targeting. Moreover, the efficacy of a chemotherapeutic drug conjugated to the vector is shown. However, more optimization may be required to achieve the full potential of the vector. The current work adds further proof for development of delivery vectors based on the conjugation of a targeting moiety and a CPP.

■ ASSOCIATED CONTENT

Supporting Information

Figure S1: Association of the FAM-labeled gHo with U87, HeLa, and HEK cells, small magnification images. Figure S2: Cellular internalization of FAM-labeled pVEC in different C- and N-terminal configurations with gHo, in U87 glioma cells, small magnification images. Figures S3 and S4: Localization of FAM-labeled gHo, pVEC, gHoPe2, and gHoPe3 in intracranial gliomas, intact brain, liver, kidney, muscle, lung, heart, skin, and spleen. Figure S5: Assessment of toxicity of FAM-labeled chimeric peptides in U87 cells (MTS and LDH assay). Figure S6: Scheme of doxorubicin-gHoPe2 (dox-gHoPe2) and HPLC traces of the synthesis reaction. Figure S7: Relative weights of the animals with intracranial tumors after the treatment with

doxorubicin and dox-gHoPe2. This material is available free of charge via the Internet at <http://pubs.acs.org>.

AUTHOR INFORMATION

Corresponding Author

*Tel: +372 737 4871. E-mail: Kaido.Kurrikoff@ut.ee.

Author Contributions

Ü.L., J.H., and P.L. designed research; K.K., E.E., J.S., N.O., D.M.C., and S.J. performed research; K.K. analyzed data; and K.K. wrote the paper.

Author Contributions

*E. E. and K. K. contributed equally to this work.

Notes

The authors declare no competing financial interest.

ACKNOWLEDGMENTS

The work was supported by Cepep III AB, by the Estonian Government through the targeted financing SF0180027s08, by the EU through the European Regional Development Fund through the Centre of Excellence of Chemical Biology, and project Tumor-Tech (SLOT112108T), by the Swedish Research Council (VR-NT) and by Cancerfoundation, Sweden. D.M.C. was supported by ESF DoRa8 programme. We thank Imre Mäger for assisting with the image processing, and we thank Helin Räägel and Prof Margus Pooga for assisting with confocal microscopy.

ABBREVIATIONS

BSA, bovine serum albumin; CPP, cell-penetrating peptide; DAPI, 4'-6-diamidino-2-phenylindole; DMEM, Dulbecco's Modified Eagle Medium; DMSO, dimethyl sulfoxide; dox, doxorubicin; FAM, 5(6)-carboxyfluorescein; FBS, fetal bovine serum; Fmoc, N-fluorenylmethoxycarbonyl; HKR, Hepes-buffered Krebs-Ringer solution; HPLC, high-performance liquid chromatography; i.p., intraperitoneal; i.v., intravenous; LDH, lactate dehydrogenase; MALDI-TOF, matrix-assisted laser desorption/ionization, time-of-flight; MBHA, methylbenzylhydramine; MTS, 3-(4,5-dimethylthiazol-2-yl)-5-(3-carboxymethoxyphenyl)-2-(4-sulfophenyl)-2H tetrazolium; Opti-MEM, reduced serum Eagle's Minimum Essential Media; PBS, phosphate buffered saline; pVEC, VE-cadherin-derived cell-penetrating peptide; s.c., subcutaneous; SMCC, succinimidyl-4-(N-maleimidomethyl)cyclohexane-1-carboxylate; TEA, triethylamine; TFA, trifluoroacetic acid.

REFERENCES

- (1) Kratz, F., Senter, P., and Steinhagen, H. (2012) *Drug Delivery in Oncology: From Basic Research to Cancer Therapy*, Wiley-VCH Verlag GmbH & Co. KGaA.
- (2) Ohgaki, H., and Kleihues, P. (2005) Population-based studies on incidence, survival rates, and genetic alterations in astrocytic and oligodendroglial gliomas. *J. Neuropathol. Exp. Neurol.* 64, 479–89.
- (3) Siegal, T., Horowitz, A., and Gabizon, A. (1995) Doxorubicin encapsulated in sterically stabilized liposomes for the treatment of a brain tumor model: biodistribution and therapeutic efficacy. *J. Neurosurg.* 83, 1029–1037.
- (4) Kurrikoff, K., Suhorutšenko, J., and Langel, Ü. (2012) Cell-Penetrating Peptides in Cancer Targeting, in *Drug Delivery in Oncology: From Basic Research to Cancer Therapy* (Kratz, F., Senter, P., and Steinhagen, H., Eds.) pp 1189–1217, Wiley-VCH Verlag GmbH & Co. KGaA.

- (5) Pasqualini, R., Koivunen, E., and Ruoslahti, E. (1997) Alpha v integrins as receptors for tumor targeting by circulating ligands. *Nat. Biotechnol.* 15, 542–6.
- (6) Essler, M., and Ruoslahti, E. (2002) Molecular specialization of breast vasculature: A breast-homing phage-displayed peptide binds to aminopeptidase P in breast vasculature. *Proc. Natl. Acad. Sci. U.S.A.* 99, 2252–2257.
- (7) Myrberg, H., Zhang, L. L., Mäe, M., and Langel, Ü. (2008) Design of a tumor-homing cell-penetrating peptide. *Bioconjugate Chem.* 19, 70–75.
- (8) Langel, Ü. (2011) Cell-Penetrating Peptides. *Methods and Protocols. Methods in Molecular Biology*, p 683, Humana Press.
- (9) Ezzat, K., El Andaloussi, S., Abdo, R., and Langel, Ü. (2010) Peptide-based matrices as drug delivery vehicles. *Curr. Pharm. Des.* 16, 1167–1178.
- (10) El-Andaloussi, S., Holm, T., and Langel, Ü. (2005) Cell-penetrating peptides: mechanisms and applications. *Curr. Pharm. Des.* 11, 3597–611.
- (11) Elmquist, A., Lindgren, M., Bartfai, T., and Langel, Ü. (2001) VE-cadherin-derived cell-penetrating peptide, pVEC, with carrier functions. *Exp. Cell Res.* 269, 237–44.
- (12) Lundin, P., Johansson, H., Guterstam, P., Holm, T., Hansen, M., Langel, Ü., and El Andaloussi, S. (2008) Distinct uptake routes of cell-penetrating peptide conjugates. *Bioconjugate Chem.* 19, 2535–42.
- (13) Elmquist, A., Hansen, M., and Langel, Ü. (2006) Structure-activity relationship study of the cell-penetrating peptide pVEC. *Biochim. Biophys. Acta* 1758, 721–9.
- (14) Fields, G. B., and Noble, R. L. (1990) Solid phase peptide synthesis utilizing 9-fluorenylmethoxycarbonyl amino acids. *Int. J. Pept. Protein Res.* 35, 161–214.
- (15) Liang, J. F., and Yang, V. C. (2005) Synthesis of doxorubicin-peptide conjugate with multidrug resistant tumor cell killing activity. *Bioorg. Med. Chem. Lett.* 15, 5071–5.
- (16) Simberg, D., Duza, T., Park, J. H., Essler, M., Pilch, J., Zhang, L. L., Derfus, A. M., Yang, M., Hoffman, R. M., Bhatia, S., Sailor, M. J., and Ruoslahti, E. (2007) Biomimetic amplification of nanoparticle homing to tumors. *Proc. Natl. Acad. Sci. U.S.A.* 104, 932–936.
- (17) Laakkonen, P., Akerman, M. E., Biliran, H., Yang, M., Ferrer, F., Karpanen, T., Hoffman, R. M., and Ruoslahti, E. (2004) Antitumor activity of a homing peptide that targets tumor lymphatics and tumor cells. *Proc. Natl. Acad. Sci. U.S.A.* 101, 9381–9386.
- (18) Agemy, L., Friedmann-Morvinski, D., Kotamraju, V. R., Roth, L., Sugahara, K. N., Girard, O. M., Mattrey, R. F., Verma, I. M., and Ruoslahti, E. (2011) Targeted nanoparticle enhanced proapoptotic peptide as potential therapy for glioblastoma. *Proc. Natl. Acad. Sci. U. S. A.* 108, 17450–5.
- (19) Rousselle, C., Clair, P., Lefauconnier, J. M., Kaczorek, M., Scherrmann, J. M., and Temsamani, J. (2000) New advances in the transport of doxorubicin through the blood-brain barrier by a peptide vector-mediated strategy. *Mol. Pharmacol.* 57, 679–686.
- (20) Mäe, M., Myrberg, H., El-Andaloussi, S., and Langel, Ü. (2009) Design of a tumor homing cell-penetrating peptide for drug delivery. *International Journal of Peptide Research and Therapeutics* 15, 11–15.